Influence of physical parameters of solar panels on infrared feature of a satellite

Wu Xiaodi, Huang Chaochao, Wang Yicheng, Yang Hua

(1. Key Lab of Infrared and Low Temperature Plasma of Anhui Province, Electronic Engineering Institute, Hefei 230037, China;
2. State Key Laboratory of Pulsed Power Laser Technology(Electronic Engineering Institute), Hefei 230037, China)

Abstract: The present literatures have not analyzed the influence of satellite's physical parameters changing with the temperature on its infrared feature. First, the theoretical calculation models of the satellite's temperature field were established. Second, the calculation method of the satellite's temperature field was deduced with the use of the finite element method (FEM) when physical parameters of solar panels changed with the temperature. Third, the calculation models of the satellite's infrared radiant emittance and its infrared radiant intensity were established. Finally, the influence of physical parameters of solar panels changing with the temperature on the surface temperature, infrared feature and the spatial distributions of infrared radiation intensities in 3-6 μm band and in 6-16 μm band of the satellite were calculated and analyzed. The research results of this paper have referential value on the improving calculation precision of infrared feature and infrared detecting of spatial targets.

Key words: earth satellite; temperature distribution; physical parameter; infrared feature
CLC number: V231.95; TN21 Documnet code: A Article ID: 1007-2276(2013)08-1962-05

太阳翼物性参数对卫星红外特性的影响

吴晓迪，黄超超，王一程，杨 华

（1. 电子工程学院 安徽省红外与低温等离子体重点实验室，安徽 合肥 230037；
2. 脉冲功率激光技术国家重点实验室(电子工程学院)，安徽 合肥 230037）

摘 要：针对现有文献在卫星红外特性研究时忽略其物性参数随温度变化对红外特性的影响，首先建立了卫星温度场的理论计算模型；然后利用有限元法进一步推导了卫星太阳翼的物性参数随温度变化时卫星温度场的求解方法；接着建立了卫星红外辐射出射度与红外辐射强度空间分布的计算模型；最后计算分析了太阳翼物性参数随温度变化对自身温度和红外特性以及对卫星整体在 3~6 μm 和 6~16 μm 两个波段红外辐射强度空间分布的影响。文章的研究结果对于提高空间目标红外特性的计算精度以及空间目标的红外探测具有参考价值。

关键词：地球卫星； 温度分布； 物性参数； 红外特性

收稿日期：2012-12-10； **修订日期**：2013-01-25

基金项目：安徽省红外与低温等离子体重点实验室项目(2011A1026)

作者简介：吴晓迪(1980-)，男，讲师，博士，主要研究方向为目标与背景的热红外特性与红外热像仿真。

Email：wuxiaodi195@sina.com

0 Introduction

With the extension of the military combat range, the amount of spatial targets increases rapidly. Infrared detecting has become an effective method for detecting spatial targets[1-2]. Thus analysis of infrared feature for spatial targets has great value and significanc[3-5]. Taking a satellite as the research object, the present literatures have not analyzed the influence of satellite's physical parameters changing with the temperature on its infrared feature [4-5]. So the theoretical calculation models are built up for a satellite's temperature field and further the calculation method of the temperature field is deduced with the use of FEM when physical parameters of its solar panels change with the temperature, as well as the influence of physical parameters of solar panels changing with the temperature on the surface temperature and the infrared radiation feature of the satellite is analyzed in detail.

1 Heat balance equations and solving process with the use of FEM

In Fig.1, the three-dimensional sectional view of the satellite is sketched. l_s and $\mathbf{d}_s$ are the length of side and the thickness of the satellite's body. l_{c1} and l_{c2} are the length and the width of the solar panel. $\mathbf{d}_c$ is the thickness of the solar panel. Γ_1 and Γ_2 are the outer interface and the inner interface of the satellite. The structural parameters are: l_s=1 m, $\mathbf{d}_s$=0.01 m, l_{c1}=4 m, l_{c2}=1 m, $\mathbf{d}_c$=0.01 m.

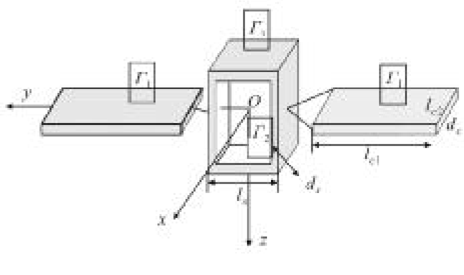

Fig.1 Sectional view of the satellite

The heat exchange of the satellite in orbit only consists of heat conduction and thermal radiation. The three-dimensional heat conduction process of the satellite is got by Eq.(1), where ρ is the material density of the satellite, **c** is the specific heat, **k** is the thermal conductivity, **T** is the temperature and t is the time.

$$\rho \mathbf{c}\frac{\partial \mathbf{T}}{\partial t}=\frac{\partial}{\partial \mathbf{x}}(\mathbf{k}\frac{\partial \mathbf{T}}{\partial \mathbf{x}})+\frac{\partial}{\partial \mathbf{y}}(\mathbf{k}\frac{\partial \mathbf{T}}{\partial \mathbf{y}})+\frac{\partial}{\partial \mathbf{z}}(\mathbf{k}\frac{\partial \mathbf{T}}{\partial \mathbf{y}}) \quad (1)$$

The boundary condition on outer interface Γ_1 of the satellite is got by Eq.(2), where $\mathbf{n}_{1x}$, $\mathbf{n}_{1y}$, $\mathbf{n}_{1z}$ are the **x**, **y**, **z** axial cosine components of the outward unit normal, the subscript 1 of **n** denotes Γ_1, α is solar radiation absorptivity, ε is infrared emissivity, η is photoelectric transformation efficiency of solar battery. If outer interface of the satellite is not the solar battery, η equals 0. $\mathbf{T}_s$ is the temperature of the spatial background. $\mathbf{E}_S$, $\mathbf{E}_{SE}$ and $\mathbf{E}_E$ are solar heat flux, earth albedo heat flux and earth heat flux, which the satellite gets, and the calculation methods for them can be got in literatures[6].

$$(\mathbf{k}\frac{\partial \mathbf{T}}{\partial \mathbf{x}}\mathbf{n}_{1x}+\mathbf{k}\frac{\partial \mathbf{T}}{\partial \mathbf{y}}\mathbf{n}_{1y}+\mathbf{k}\frac{\partial \mathbf{T}}{\partial \mathbf{z}}\mathbf{n}_{1z})|_{\Gamma_1}=(\alpha \mathbf{E}_S+\alpha \mathbf{E}_{SE})(1-\eta)+ \varepsilon \mathbf{E}_E+\varepsilon\sigma(\mathbf{T}_s^4-\mathbf{T}^4) \quad (2)$$

The boundary condition on inner interface $\mathbf{F}_2$ of the satellite is got by Eq.(3), where $\mathbf{q}_{net}$ is the net radiation density which can be got by Gebhart method, $\mathbf{q}_{inner}$ is radiation density of the inner heat source.

$$(\mathbf{k}\frac{\partial \mathbf{T}}{\partial \mathbf{x}}\mathbf{n}_{2x}+\mathbf{k}\frac{\partial \mathbf{T}}{\partial \mathbf{y}}\mathbf{n}_{2y}+\mathbf{k}\frac{\partial \mathbf{T}}{\partial \mathbf{z}}\mathbf{n}_{2z})|_{\Gamma_2}=\mathbf{q}_{net}+\mathbf{q}_{inner} \quad (3)$$

Discretizing the solution domain into a number of finite elements and using the weighted residual method, one can obtain finite element matrix equation of heat conduction process with boundary conditons in the global solution domain. In the finnite element matrix equation of Eq.(4), [C] is heat capacity matrix, [K] is heat conductivity matrix, {P} is load vector, {T} is the nodal temperature vector, $\{\dot{T}\}$ is the vector of nodal temperature derivative with respect to time.

$$[C]\{\dot{T}\}+[C](\mathbf{T})]\{T\}=\{P\} \quad (4)$$

Eq.(4) suppose the satellite's physical parameters do not change with the temperature, such as the specific heat and the thermal conductivity **k**. In fact, these parameters always change with the temperature. So the finite element matrix equation should be Eq.(5), where the heat capacity matrix $[C(\mathbf{T})]$ and the heat conductivity matrix $[K(\mathbf{T})]$ change with the temperature.

$$[C(\mathbf{T})]\{\dot{T}\}+[K(\mathbf{T})]\{T\}=\{P\} \tag{5}$$

With the use of the interpolation method, one can obtain Eq.(6), where the subscript **n** and **n**+1 denote the time t_n and t_{n+1}, $\mathbf{N}_n=(t_{n+1}-t)/\Delta t$, $\mathbf{N}_{n+1}=(t-t_n)/\Delta t$, $\dot{\mathbf{N}}_n=-1/\Delta t$, $\dot{\mathbf{N}}_{n+1}=-1/\Delta t$, $\Delta t=t_{n+1}-t_n$.

$$[C(\mathbf{T})]\approx \mathbf{N}_n[\mathbf{C}_n]+\mathbf{N}_{n+1}[C_{n+1}]$$

$$\{\dot{T}\}\approx \dot{\mathbf{N}}_n\{T_n\}+\dot{\mathbf{N}}_{n+1}\{T_{n+1}\}$$

$$[K(\mathbf{T})]\{T\}\approx \mathbf{N}_n([\mathbf{K}_n]\{T_n\}+\mathbf{N}_{n+1}[\mathbf{K}_{n+1}]\{T_{n+1}\})$$

$$\{P\}\approx \mathbf{N}_n\{P_n\}+\mathbf{N}_{n+1}\{P_{n+1}\} \tag{6}$$

With the use of Eq.(6) and the weighted residual method, one can get Eq.(7) from Eq.(5).

$$\left(\frac{[C_n]}{\Delta t}+\left(\frac{[C_{n+1}]}{\Delta t}-\frac{[C_n]}{\Delta t}+[K_{n+1}]\right)\theta\right)\{T_{n+1}\}=$$

$$\left(\frac{[C_n]}{\Delta t}+\left(\frac{[C_{n+1}]}{\Delta t}-\frac{[C_n]}{\Delta t}\right)\theta-[K_n](1-\theta)\right)\{T_n\}+$$

$$\{P_n\}(1-\theta)+\{P_{n+1}\}\theta \tag{7}$$

With the use of the Galerkin method and the iterative method, the temperature field of the satellite can be got from Eq.(7). In the calculation process the value of θ is 2/3.

2 IR radiation feature calculation

The infrared radiant emittance $\mathbf{M}_{dA_i}$ of the satellite's surface differential area $\mathbf{dA}_i$, which consists of the self radiant emittance $\mathbf{M}_{dA_i,s}$ and the reflected radiant emittance $\mathbf{M}_{dA_i,r}$, is got by Eq.(8). The calculation methods of $\mathbf{M}_{dA_i,s}$ and $\mathbf{M}_{dA_i,r}$ can be obtained from the literature[7].

$$\mathbf{M}_{dA_i}=\mathbf{M}_{dA_i,s}+\mathbf{M}_{dA_i,r} \tag{8}$$

Figure 2 shows the coordinate system in which IR radiant intensity of the satellite is calculated. The orthogonal axes respectively have the same directions with the corresponding axes in the geocentric equatorial inertial coordinate system.

The satellite is assumed to be diffusing grey body. IR radiant intensity of the satellite in the direction indicated by θ_{IR} and Φ_{IR} can be got by Eq.(9).

$$\mathbf{I}_{\theta_{IR},\Phi_{IR}}=\sum_{i=1}^{N}\left(\frac{1}{\pi}\mathbf{M}_{dA_i,s}\mathbf{dA}_i\right)(\hat{\mathbf{n}}_{dA_i}\cdot\hat{\mathbf{n}}_{\theta_{IR},\Phi_{IR}})+$$

$$\sum_{i=1}^{N}\left(\frac{1}{\pi}\mathbf{M}_{dA_i,r}\mathbf{dA}_i\right)(\hat{\mathbf{n}}_{dA_i}\cdot\hat{\mathbf{n}}_{\theta_{IR},\Phi_{IR}}) \tag{9}$$

where the subscript i denotes the index of partitioned surface elements of the satellite, $\hat{\mathbf{n}}_{dA_i}$ is the outward unit normal vector of the surface differential area $\mathbf{dA}_i$, $\hat{\mathbf{n}}_{\theta_{IR},\Phi_{IR}}$ is the outward unit normal vector and $\hat{\mathbf{n}}_{\theta_{IR},\Phi_{IR}}=\{\sin\theta_{IR}\cos\Phi_{IR},\sin\theta_{IR}\sin\Phi_{IR},\cos\theta_{IR}\}$.

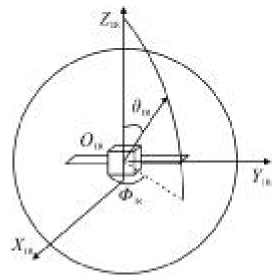

Fig.2 IR radiant intensity calculation

3 Numerical results and discussions

In Fig.1, the satellite is three-axis stabilized which is in the sun-synchronous orbit. $\pm$**y** surfaces are radiating surfaces and the others are covered with the multi-layer heat-barrier material. $\pm$**x** axis points to motion direction of the satellite and $\pm$**z** axis points to geocenter. The obverse side of solar panels which has cell battery is always oriented towards the sun in the sunshine and towards the space in the earth's shadow. The satellite orbit period is divided into 600 intervals. The orbit parameters and the physical parameters of the satellite's body can be obtained from the literature [8]. The temperature distribution and infrared feature of the satellite's body has been also calculated and analyzed in the same literature, so in this paper the influence of physical parameters of solar panels changing with the temperature on its surface temperature, infrared feature and the spatial distributions of infrared radiation intensities in 3-6 μm band and in 6-16 μm band of the satellite is mainly calculated and analyzed. The physical parameters of solar panels changing with the temperature are: **k** =

$(0.0021\mathbf{T}+0.26)$ W/(m·K), $\mathbf{c}=(2.87\mathbf{T}+68)$J/(kg·K), $\eta=(15.8-0.068t)\%$, t is the Celsius temperature of solar panels' cell battery. The other properties can be also got in the literature [8].

In Fig.3, (a) is the surface temperature of solar panel of which the physical parameters change with the temperature. (b) is the temperature difference between the solar panel in this paper and the solar panel of which the physical parameters do not change with the temperature in the literature [8]. As shown in Fig.3, physical parameters which change with the temperature have influence on the temperature of solar panel. In the most time of satellite orbit period, the temperature of solar panel of which the physical parameters change is higher. The temperature difference of the inverse side is greater than the obverse side's.

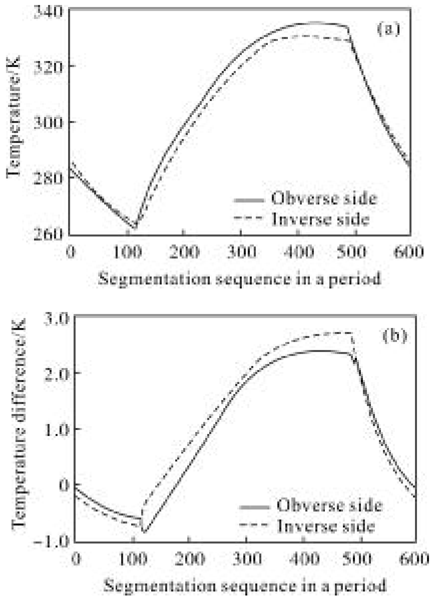

Fig.3 Surface temperature and temperature difference of solar panel

In Fig.4, (a1) and (a2) are infrared radiant exitances of solar panel of which the physical parameters change with the temperature in 3-6 μm band and 6-16 μm band, (b1) and (b2) are radiant exitance differences in two IR bands. As shown in (a1) and (a2) of Fig.4, the radiant exitances of inverse side in two IR bands descend suddenly when the satellite leaves the earth's shadow area and just comes into the sunshine area. This is because in the earth's shadow area the inverse side is always towards the earth and reflects much earth radiation, but in the sunshine area the inverse side isn't towards the earth and reflects less earth radiation because of the obverse side which has cell battery always orienting towards the sun at the moment. By the same token, the reason of the inverse side's infrared radiant exitances rising suddenly when the satellite leaves the sunshine area and just comes into the earth's shadow area is the inverse side reflecting more earth radiation in the earth's shadow area than ones in the sunshine area. As shown in (b1) and (b2) of Fig.4, one can find radiant exitances in two IR bands are enhanced in the most time of satellite

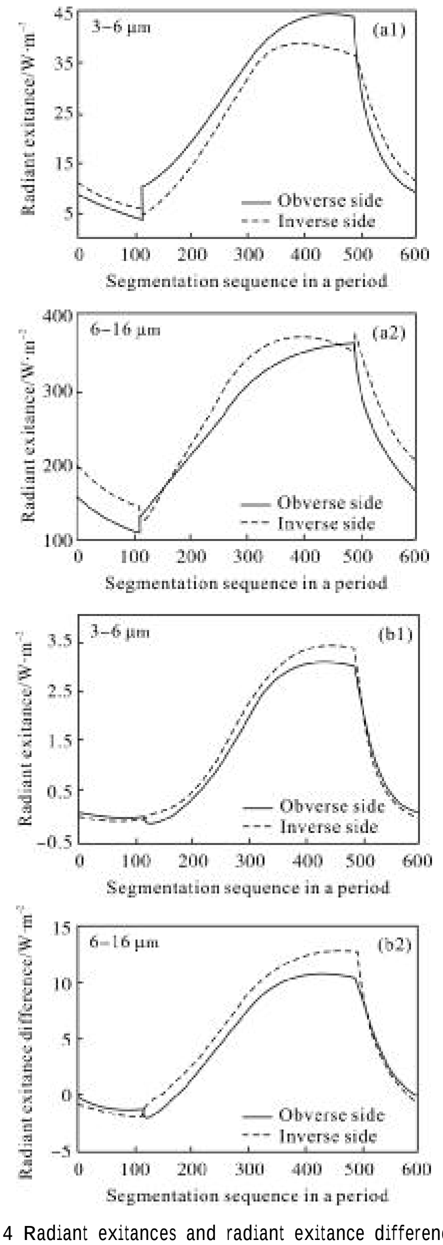

Fig.4 Radiant exitances and radiant exitance differences of solar panel in two IR bands

orbit period and the radiant exitance difference in 6-16 μm band is greater than the one in 3-6 μm band.

In Fig.5, (a1) is the spatial distribution of radiant intensity in 3-6 μm band of the satellite at the 435th interval of the satellite's orbit period. At this moment the radiant intensity difference in 3-6 μm band is the greatest. As shown in (b1), the greatest difference is 6.348 3 W/sr. (a2) is the spatial distribution of radiant intensity in 6-16 μm band at the 448th interval. The radiant intensity difference in 6-16μm band is the greatest at preasent and the greatest difference is 32.595 0 W/sr which is shown in (b2).

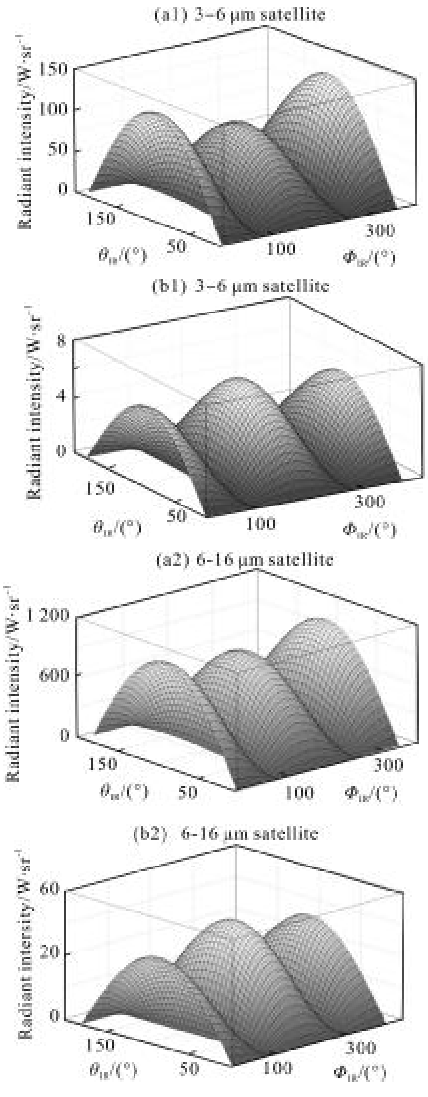

Fig.5 Spatial distributions of radiant intensities and radiant intensities differences of satellite in two IR bands

4 Conclusions

According to the calculation results, one can find that physical parameters of solar panels changing with the temperature have the influence on the surface temperature, infrared feature and the spatial distributions of infrared radiation intensities in 3-6 μm band and in 6-16 μm band. The influence on the infrared feature of the satellite in 6-16 μm band is more distinct than the one in 3-6 μm band. So in the calculation of spatial targets' infrared feature the influence on their infrared feature which is caused by physical parameters changing with the temperature should be analyzed. The research results of this paper have referential value on the improving calculation precision of infrared feature and infrared detecting of spatial targets.

References:

[1] Heinisch Roger P, Jolliffe Clinton L, Schmidt Roger N. An experimental and analytical study of visual detection in a spacecraft environment [R]. United States: NASA CR-1561, 1970: 1-4

[2] Tidrow M Z, Dyer W R. Infrared sensors for ballistic missile defense [J]. Infrared Physics & Technology, 2001, 42(3/5): 333-336.

[3] Guo Lixin, Zhao Kang. Study on the characteristic of IR radiation from the space target [J]. International Journal of Infrared and Millimeter Waves, 2004, 25(1): 119-127.

[4] Shi Liangchen, Zhu Dingqiang, Cai Guobiao. Simulation research of multi-spectral signature of satellite [J]. Opto-Electronic Engineering, 2009, 36(5): 40-45. (in Chinese)
石良臣, 朱定强, 蔡国飙. 卫星多光谱信号的仿真研究[J]. 光电工程, 2009, 36(5): 40-45.

[5] Han Yuge, Xuan Yimin. Infrared feature of the satellite [J]. Infrared and Laser Engineering, 2005, 34(1): 34-37. (in Chinese)
韩玉阁, 宣益民. 卫星的红外辐射特征研究 [J]. 红外与激光工程, 2005, 34(1): 34-37.

[6] Zhang Jun. Finite element analysis of the surface temperature distribution on the exoatmospheric ballistic target[J]. Infrared and Laser Engineering, 2008, 37(3): 416-419. (in Chinese)

[7] Wu Xiaodi. Surface Temperature Distribution and Infrared Radiation Feature of a Spatial Balloon Decoy [C]. International Symposium on Photoelectronic Detection and Imaging 2009, 2009: 73831M.

[8] Wu Xiaodi. Infrared Feature of a satellite and influence of spatial heat flux on it [J]. Opto-Electronic Engineering, 2010, 37(6): 58-64. (in Chinese)